

# DESIGN AND STRUCTURAL ANALYSIS OF A TIMBER SHELL STRUCTURE USING RFEM AND GRASSHOPPER

**C.O. Bakker**

MSc student, Department of Civil Engineering, Track Structural Engineering, Delft University of Technology (TU Delft), Stevinweg 1, 2628 CN Delft, The Netherlands, [cobakker@student.tudelft.nl](mailto:cobakker@student.tudelft.nl)

## ABSTRACT

*This paper presents a comprehensive study on the design, modeling and analysis of a timber shell structure, emphasizing the sustainability, aesthetic appeal and structural performance of timber as a construction material. Utilizing advanced computational tools such as Rhinoceros (Rhino), Grasshopper (GH) and RFEM, the study explores innovative form-finding techniques and interactive physics simulations to optimize the structure's geometry and performance.*

*The design phase draws inspiration from notable timber shell structures and incorporates key architectural and structural considerations. The initial analysis identified several areas where the structure did not meet the required safety and serviceability standards, particularly in terms of bending, combined bending and compression and maximum deformations.*

*To address these issues, two improvement options were proposed. The first option involved increasing the cross-sectional dimensions drastically, while the second option included increasing the edges and adding diagonals, along with resizing the inner members. The final analysis demonstrated that these modifications significantly enhanced the structural performance, ensuring compliance with all relevant criteria.*

*The results highlight the importance of iterative design and analysis in achieving a safe, efficient and sustainable timber shell structure. This study underscores the potential of timber as a versatile and environmentally friendly construction material and the effectiveness of advanced computational tools in modern structural engineering.*

**Keywords:** Timber shell structure, Structural analysis, Computational modeling, Rhinoceros (Rhino), Grasshopper (GH), RFEM, Form-finding, Sustainable construction, Structural performance, Architectural design.

## 1. INTRODUCTION

The design and analysis of timber structures have gained significant attention in recent years due to their sustainability, aesthetic appeal and structural performance. Timber, as a renewable and environmentally friendly material, offers a compelling alternative to traditional construction materials like steel and concrete. This paper presents a comprehensive study on the design, modeling and analysis of a timber shell structure, utilizing advanced computational tools to optimize its performance.

The structure of the paper is as follows. The **Design Intention** section outlines the conceptual sketches and design principles. The

**Modelling of Geometry** section describes the process of creating the geometric model using Rhinoceros (Rhino) and Grasshopper (GH). The **Description of Analysis** section details the analytical methods used to evaluate structural performance, including static and load assessments.

The **Results** section is divided into three parts: **Initial Results**, which highlights areas where the structure did not meet standards; **Improvements**, which discusses proposed modifications and their impact; and **Final Results**, which summarizes the results after improvements, demonstrating compliance with all criteria.

The **Discussion** section outlines the remarkable parts of the project, items that were left out and the opinion on the applied techniques. The **Conclusion** chapter provides a summary of the study, emphasizing the effectiveness of advanced computational tools and the potential of timber as a sustainable construction material.

## 2. DESIGN INTENTION

The design process began with researching timber shell structures and the common shapes used in such constructions. The timber shell structures by Chalmers University of Technology and Edinburgh Napier University served as a base for the shape, figure 1 and 2 respectively [1][2]. Since the shell structure is to be placed on the roof of a building, it is crucial to consider how the forces are transmitted to the ground. The first decision made was that the supports, or the edges connected to the ground, should be positioned on or very close to the columns used in the building structure below.



**Figure 1:** Timber shell structure by Chalmers UoT  
(Photo:©Designboom.com)



**Figure 2:** A bamboo grid shell structure by Edinburgh Napier University (Photo: © Edinburgh Napier University)

As depicted in Figure 3, the structure consists of timber beams arranged in a parabolic configuration. The side view illustration shows the curvature of the timber shell, supported at the edges and spanning

across the roof. The placement of the supports directly above the columns of the substructure ensures efficient load transfer, minimising structural stress and enhancing stability.

The top view sketch, Figure 4, reveals a unique design feature: a central circular opening. This opening not only improves sunlight penetration but also enhances the dynamic visual appeal of the structure. The circular void introduces a sense of openness and allows natural light to filter through, creating an inviting and well-lit space below.

To protect the structure from environmental elements such as rain and snow, sheets of extruded polycarbonate are used as a cover. These sheets are chosen for their durability, transparency and resistance to impact, providing effective protection while allowing light to pass through. The use of polycarbonate ensures that the interior remains dry and safe from weather conditions, enhancing the longevity and functionality of the timber shell.

Overall, the design integrates aesthetic considerations with practical engineering solutions. The use of timber slats or short beams arranged in a parabolic form not only provides structural efficiency but also showcases the natural beauty of the material. The design's attention to light, space and structural coherence reflects a thoughtful and innovative approach to timber architecture.

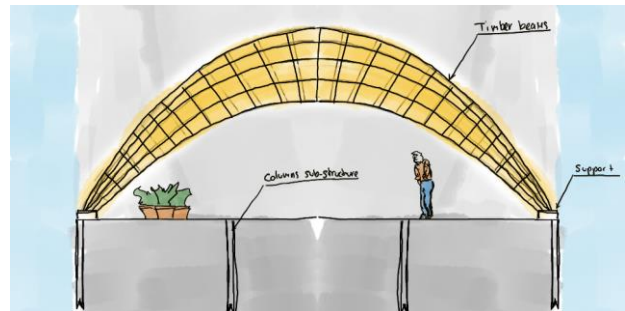


**Figure 3:** Sketch side structure

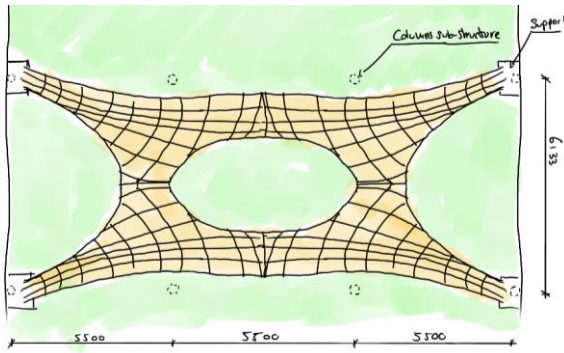


**Figure 4:** Sketch top structure

### 3. MODELLING OF GEOMETRY

The project explores advanced form-finding techniques using Rhino and Grasshopper, with a focus on achieving fully compressive structures. The process and final outcome are illustrated through a series of images, showcasing the steps taken to create an optimized mesh structure.

Initially, a basic shape was created in Rhino, consisting of a rectangle with a circular cut-out in the middle. This shape was then remeshed using the QuadRemesh tool to generate a mesh composed of quadrilateral faces, providing a more uniform and manageable structure.

For the form-finding process, the Kangaroo2 plugin in Grasshopper was employed. Kangaroo2 is a powerful tool for interactive physics simulation, essential for determining the shape of structures under various forces. Three key components were utilised: EdgeLength, Load and Anchor.

The EdgeLength component was crucial in maintaining or adjusting the lengths of the mesh edges, allowing for control over the tension within the mesh. By fine-tuning the Strength and LengthFactor parameters, the desired edge lengths and tension were achieved, ensuring the mesh's structural integrity.

The Load component simulated gravity forces acting on the mesh. Adjusting the Weighting parameter controlled the magnitude of these forces, helping to find an equilibrium shape under load.

The Anchor component set the positions of the support points, defining the boundary conditions of the structure.

Through iterative adjustments of the EdgeLength and Load parameters, the preferred shape, fully in compression, was found. This process ensured that the final structure was both efficient and aesthetically pleasing.

The figures below illustrate various views of the final mesh structure:

- Figure 5 provides a 3D perspective view, highlighting the overall form and the applied mesh pattern.
- Figure 6 presents a top view with dimensions, showing the layout and positioning of the support points and the mesh grid.
- Figure 7 offers a front view, detailing the profile of the structure, including its height and span.
- Figure 8 displays another side view from a different angle, providing a clear perspective on the curvature and elevation of the structure.

The result is an optimised mesh structure that efficiently carries loads through compression, demonstrating the potential of advanced form-finding techniques in civil engineering applications.



**Figure 5:** 3D model structure



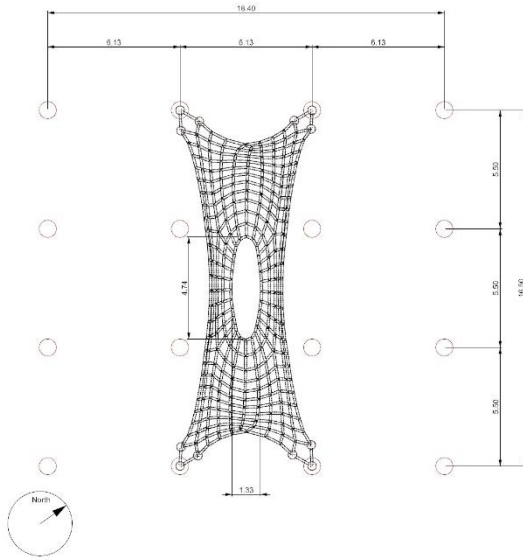


Figure 6: Dimensions top structure

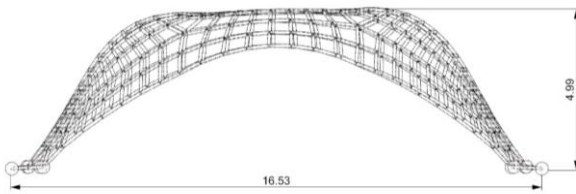


Figure 7: Dimensions side structure

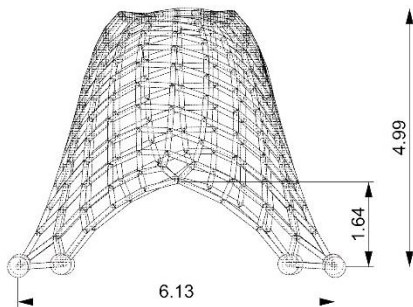


Figure 8: Dimensions front structure

#### 4. DESCRIPTION OF ANALYSIS

The type of analysis used by the RFEM 6 software is geometrically linear. This means that the equilibrium is analysed on an undeformed structural system. A linear analysis is carried out because deformations of the components are not included in the calculation. The loads that are active on the structure are the

permanent load, the wind load and the snow load.

The permanent load takes into account the self-weight of the timber beams, dependent on the cross section and timber choice. As well as the weight of the extruded polycarbonate sheets. The weight of the sheets is 0.12 kN per square meter.

As RFEM 6 works with member loads a calculation has to be made to change the load from per square meter to per meter per element. The average length of the members,  $\bar{n}$ , is 0.61 meter. The load in between four members is therefore:  $q * \bar{n} * \bar{n}$  kN. The distributed load per member is stated in equation 1. This formula is used for the load from the sheets, wind load and snow load.

$$q_{member} = \frac{q[kN] * \bar{n}^2}{4} * 2 * \frac{1}{\bar{n}} = \frac{q * \bar{n}}{2} \left[ \frac{kN}{m} \right] \quad (1)$$

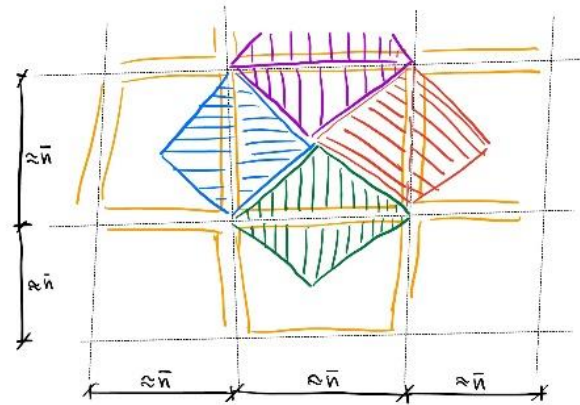


Figure 9: Load distribution members

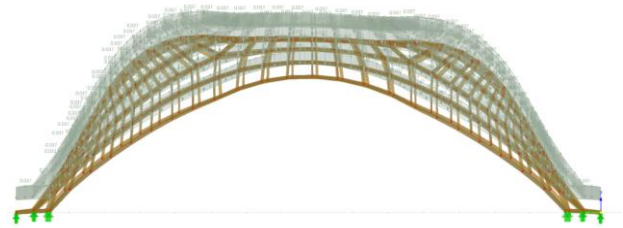


Figure 10: Permanent load RFEM

The wind load is calculated is calculated in the same manner as the uniform permanent load of the sheets. The wind load is mainly present on the short side of the structure, shown in Figure 7, as the two towers are placed next to the structure on either side from this angle. Therefore this is the angle in which the wind load is considered. For the first half of the

structure the wind load is considered positive and works on the outside of the structure, for the second half the wind load is considered negative and works on the inside of the structure. The wind load works in the direction of the local z-axis of the beams. This means perpendicular to the span of the beam. The height of the middle part of the building is 9.7 meter and the height of the structure itself is 4.99 meter. The peak velocity pressure in area II, type: urban and height of 15 meter is: 0.8 kN per square meter. To assure safety a force coefficient factor of 1.4 is chosen for both positive and negative loads as the tunnel effect between the towers was not taken into account. The final wind load is 1.12 kN per square meter.

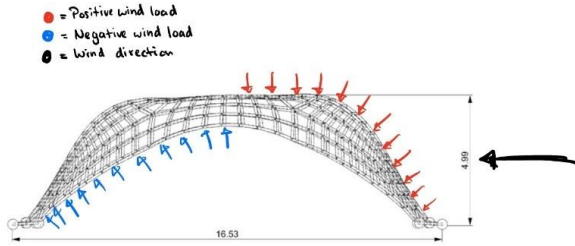


Figure 11: Windload sketch

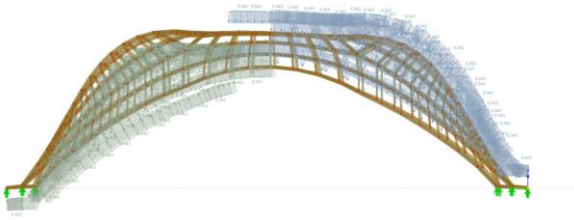


Figure 12: Wind load Rfem

The snowload is projected on the members. As the snowload cannot accumulate in the structure a shape coefficient of 0.8 is chosen, good is to keep in mind that this is still highly conservative. The characteristic value of snowload on the ground in the Netherlands is 0.7 kN per square meter. The adjusted snow load is 0.56 kN per square meter.

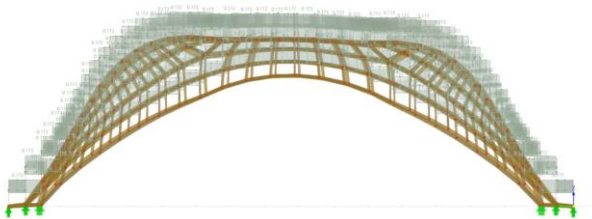


Figure 13: Snow load RFEM

Table 1: Loads on structure

Type load	Load per m2 [kN/m2]	Member load [kN/m]	Factor for combination ( $\Psi_0$ )[-]
<b>Permanent</b>	Self weight + 0.12	Self weight + 0.036	-
<b>Wind</b>	1.12	0.342	0
<b>Snow</b>	0.56	0.172	0

The consequence class for the timber shell structure is 2. As there are medium consequences for loss of human life and the consequences of failure are minimum overall. Based on the general formula for the ultimate limit state, equation 2, the four load combinations can be determined.

$$\gamma_G G_k + \gamma_{Q;1} Q_{1;k} + \sum (\gamma_{Q;i} \Psi_{0;i} Q_{i;k}) \quad (2)$$

1.  $1.2 * G_k + 1.5 * Q_{wind}$
2.  $0.9 * G_k + 1.5 * Q_{wind}$
3.  $1.2 * G_k + 1.5 * Q_{snow}$
4.  $0.9 * G_k + 1.5 * Q_{snow}$

The load combinations used for the serviceability limit state are as follows:

1.  $1.0 * G_k + 1.0 * Q_{wind}$
2.  $1.0 * G_k + 1.0 * Q_{snow}$

At the end of the modelling phase for the initial iteration, the beams of the timber shell structure are specified as C24 timber with a rectangular cross-section measuring 50 by 100 mm. The use of C24 timber, a common structural grade in timber engineering, provides a reliable and standardized basis for further analysis and design iterations.

## 5. RESULTS

This section presents the analysis and verification of the timber shell structure's safety and serviceability. The safety assessment is based on the unity check of bending, compression combined with bending and tension combined with bending. Serviceability Limit

State (SLS) checks ensure that maximum deformation remains within the core size of the cross-section. Additionally, the beams are evaluated for buckling. The chapter is divided into three main parts. The initial results section provides the analysis of the cross-section, material and loads from the previous chapter. The improvements section details the modifications made to enhance the structure. The final results section presents the analysis of the improved structure, ensuring it meets all safety and serviceability criteria.

### 5.1 Initial results

The analysis of the timber shell structure indicates that load combination 2 leads to the highest forces within the structure. Starting with examining the Ultimate Limit State (ULS). The partial safety factor for material,  $\gamma_m$ , is used as a sawn timber section is employed. The strength modification factor  $k_h$  is calculated using the Equation 8.

$$k_h = \min\left(\left(\frac{150}{h}\right)^{0.2}, 1.3\right) \quad (3)$$

The modification factor  $k_{mod}$  is determined to be 0.80, considering that the load duration class is medium and the service class is 2. This classification is appropriate since the structure is located outside, where the average humidity in the Netherlands is 77%, exceeding the 65% threshold for service class 1.

#### Bending stress check

The maximum moment  $M_d$  in the structure is found to be 2.61 kNm. Using the bending stress Equation 4. The design bending strength is calculated using Equation 5.

$$\sigma_{m,0,d} = \frac{6M_d}{bh^2} \quad (4)$$

$$f_{m,0,d} = \frac{f_{m,k}}{\gamma_m} \cdot k_h \cdot k_{mod} \quad (5)$$

For a cross-section with a width  $b$  of 50 mm and height  $h$  of 100 mm, the bending stress  $\sigma_{m,0,d}$  is found to be 31.32 N/mm<sup>2</sup>. The unity check (UC) for bending moment is 1.96, which is too high.

#### Compression Stress Check

The maximum normal force  $N_{max}$  in the structure is 60.50 kN. Using the compression stress formula:

$$\sigma_{c,0,d} = \frac{N_{max}}{bh} \quad (6)$$

Given the cross section, , the compression stress  $\sigma_{c,0,d}$  is 12.10 N/mm<sup>2</sup>. The design compression strength  $f_{c,0,d}$  is derived from the characteristic compression strength  $f_{c,0,k}$  given Equation 7.

$$f_{c,0,d} = \frac{f_{c,0,k}}{\gamma_m} \cdot k_{mod} \quad (7)$$

Given  $f_{c,0,k} = 21$  N/mm<sup>2</sup>, the design compressive strength is  $f_{c,0,d} = 12.92$  N/mm<sup>2</sup>. The unity check (UC) for compression is 0.93, confirming the stress is within acceptable limits.

#### Combined bending and compression

The combined bending and compression stress is checked using the interaction formula. Two beams are considered: one where the moment is highest and one where the compression force is highest. The interaction formula for the unity check is split into two equations, one in which the moment over the y-axis is leading the other in which the moment over

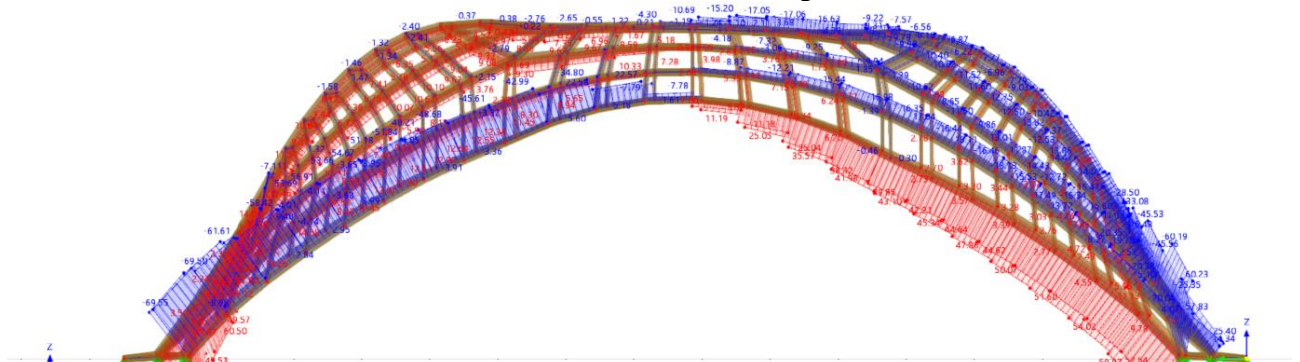


Figure 14: Normal force load combination 1

the z-axis is leading. For a rectangular cross section  $k_m = 0.7$ .

$$\left(\frac{\sigma_{c,0,d}}{f_{c,0,d}}\right)^2 + \frac{\sigma_{m,y,d}}{f_{m,y,d}} + k_m \frac{\sigma_{m,z,d}}{f_{m,z,d}} \leq 1 \quad (8)$$

$$\left(\frac{\sigma_{c,0,d}}{f_{c,0,d}}\right)^2 + k_m \frac{\sigma_{m,y,d}}{f_{m,y,d}} + \frac{\sigma_{m,z,d}}{f_{m,z,d}} \leq 1 \quad (9)$$

The unity checks for the combined stresses are given in Table 2. These results highlight that the design needs to be improved to ensure the structure's safety under the applied loads. The moment over the y-axis and z-axis are given in Figure 15 and 16 respectively.

**Table 2:** Unity check bending + compression

	$N_{max}$ dom.	$M_{max}$ dom.
$UC_{comp;y\_primary}$	2.71	4.08
$UC_{comp;z\_primary}$	2.44	4.08

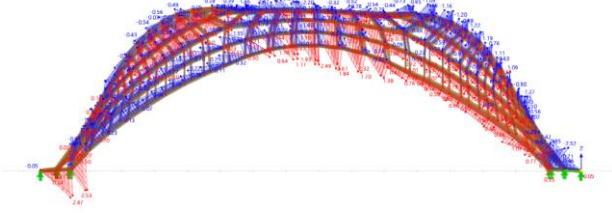


**Figure 15:** Moment y-axis

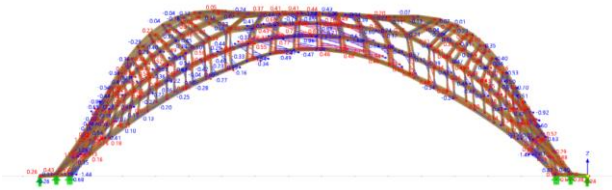


**Figure 16:** Moment z-axis

### Combined bending and tension

Similarly to the checks performed for bending and compression combined, the same verification is now carried out for bending and tension combined using the following formulas:

$$\frac{\sigma_{t,0,d}}{f_{t,0,d}} + \frac{\sigma_{m,y,d}}{f_{m,y,d}} + k_m \frac{\sigma_{m,z,d}}{f_{m,z,d}} \leq 1 \quad (10)$$

$$\frac{\sigma_{t,0,d}}{f_{t,0,d}} + k_m \frac{\sigma_{m,y,d}}{f_{m,y,d}} + \frac{\sigma_{m,z,d}}{f_{m,z,d}} \leq 1 \quad (11)$$

**Table 3:** Unity Check Bending + Tension

$UC_{tens;y\_primary}$	4.11
$UC_{tens;z\_primary}$	4.00

As shown in Table 3, the unity checks for both bending and compression combined are too high.

### Buckling

To ensure the structural integrity of the timber shell under compressive loads, a detailed buckling analysis is conducted. The critical buckling coefficient,  $k_c$ , is determined using the relative slenderness ratio,  $\lambda_{rel}$ , and the buckling factor,  $k$ .

First, the slenderness ratio  $\lambda$  is calculated as the effective length  $l_{eff}$  of the member divided by the radius of gyration  $r$ . As the members are fully restraint at both sides, the effective length is half the length of the member. To simplify the calculation the largest length (1034 mm) is taken to calculate the effective length. The radius of gyration  $r$  is a measure of the distribution of the cross-sectional area around an axis and is defined as:

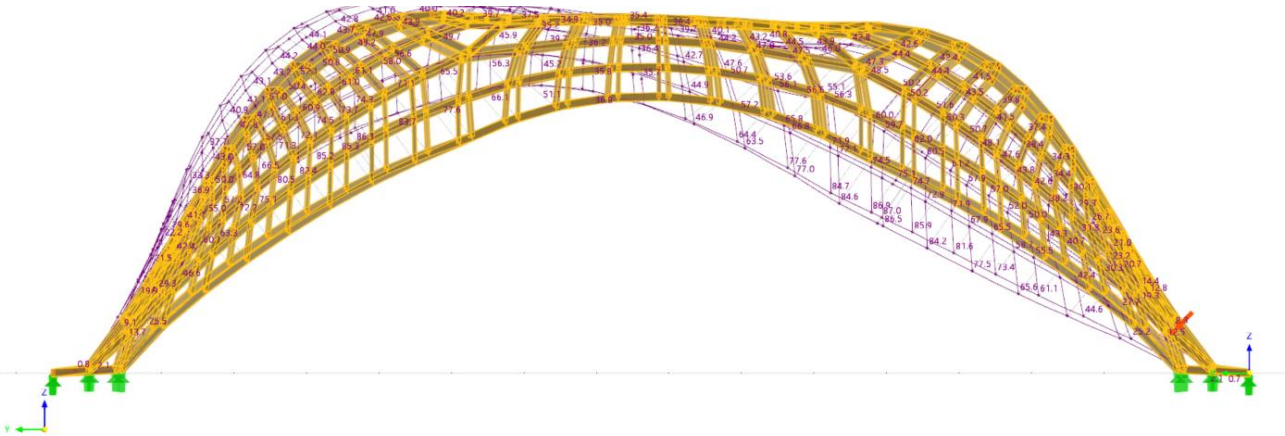
$$r = \sqrt{\frac{I}{A}} \quad (12)$$

$$\lambda = \frac{l_{eff}}{r} \quad (13)$$

The relative slenderness  $\lambda_{rel}$ , ratio then calculated as follows:

$$\lambda_{rel} = \frac{\lambda}{\pi} \sqrt{\frac{f_{c,0,k}}{E_{0.05}}} \quad (14)$$



**Figure 17:** Deformation initial design [mm]

The buckling factor  $k$  is calculated using:

$$k = 0.5(1 + \beta(\lambda_{\text{rel}} - 0.3) + \lambda_{\text{rel}}^2) \quad (15)$$

For sawn timber,  $\beta$  is 0.20.

Next the critical buckling coefficient  $k_c$  is obtained from:

$$k_c = \frac{1}{k + \sqrt{k^2 - \lambda_{\text{rel}}^2}} \quad (16)$$

Finally, the requirement for preventing buckling is checked using the following inequality:

$$\frac{\sigma_{c,0,d}}{k_c f_{c,0,d}} \leq 1 \quad (17)$$

This ensures that the design compressive stress does not exceed the buckling capacity of the timber.

**Table 4:** Buckling calculation results

Parameter	Value	Unit
$r$	28.87	mm
$l_{ef}$	517	mm
$\lambda$	17.91	[-]
$\lambda_{\text{rel}}$	0.30	[-]
$k$	0.55	[-]
$k_c$	1.00	[-]

$$UC_{\text{buckling}} = 0.94 \quad [-]$$

The values obtained from the buckling calculations are summarized in the Table 4. Notably, the unity check for buckling UC is 0.94, which indicates that the compressive stress in the members is within acceptable limits, ensuring stability against buckling.

### Deformation

For the Serviceability Limit State (SLS), the load combination with the wind (SLS load combination 1) results in the highest deformation within the structure. The primary concern for SLS is to ensure that the deflections remain within acceptable limits to maintain structural integrity and functionality.

In this analysis, the deformation is predominantly in the  $z$  and  $y$  directions. This means that the deformation is the greatest in the direction of the height of the cross section. Therefore the maximum allowable displacement is set to  $\frac{h}{6}$ . This criterion ensures that the displacement does not exceed the limits defined by the central core's dimensions, as seen in Figure 18, thereby maintaining structural stability and serviceability. For a cross-section height  $h$  of 100 mm, the allowable maximum displacement is calculated as:

$$d_{\text{allowed}} = \frac{h}{6} = 16.66 \text{ [mm]} \quad (18)$$



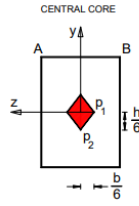


**Figure 18:** Core cross section

The maximum displacement observed in the structure is 86.5 mm, which occurs approximately one-quarter of the way from the right end of the structure, as illustrated in the Figure 17. This displacement significantly exceeds the allowable limit. The Unity Check (UC) for the displacement is calculated as the ratio of the actual displacement to the allowable displacement:

$$UC_{SLS} = \frac{d_{actual}}{d_{allowed}} = \frac{86.5}{16.66} = 5.19[-] \quad (19)$$

A UC value of 5.19 indicates that the displacement is more than five times the allowable limit, which is unacceptable and necessitates design modifications to reduce the deformation. The excessive displacement could compromise the structural performance and serviceability, highlighting the need for structural improvements.

## 5.2 Improvements

The initial analysis revealed that the Ultimate Limit State (ULS) checks for bending, the combination of bending and compression and the combination of tension and bending exceeded acceptable limits. To address these issues, two options are discussed below.

### Option 1: Increasing cross-section dimension

By increasing the cross-section from 50 mm by 100 mm to 80 mm by 190 mm for all elements, the structural capacity is significantly enhanced. This adjustment reduces the stress levels experienced by the members under load, thereby improving their performance under both bending and the combined conditions, the results can be found in Appendix 2.

Additionally, the increased cross-section has a positive impact on the SLS. The maximum deformation is reduced to 13.42 mm, which is within the new allowable displacement limit of 31.67 mm.

This adjustment ensures that the structure not only meets the safety requirements but also maintains acceptable serviceability performance, thus making the structure safe for use.

This option effectively addresses the initial shortcomings in the design, ensuring that the structural integrity and serviceability criteria are met.

### Option 2: Adding diagonals at the edges

The second option to address the structural issues is to modify the cross-sections and add additional members. Specifically, the edges are increased to 80 mm by 160 mm and diagonals of the same dimensions are added. Additionally, the inner members are increased to 60 mm by 120 mm. These changes significantly enhance the structural capacity and address the excessive unity checks observed in the initial analysis.

This adjustment ensures that all unity checks are within acceptable limits. The maximum deformation of the outer members is reduced to 19.8 mm, which is well within the allowable limit of 26.67 mm. For the inner members, the maximum deformation is 16.7 mm, staying below the allowable limit of 20 mm. These improvements ensure that the structure meets both safety and serviceability requirements, providing a robust and reliable solution.

### Choice

In conclusion, both options presented address the structural deficiencies identified in the initial analysis. However, Option 2 offers several advantages over Option 1.

Option 1 uses a total timber volume of 5.42 m<sup>3</sup>, while Option 2 uses only 3.42 m<sup>3</sup>. The significant reduction in timber volume makes Option 2 more material-efficient. This reduction not only conserves resources but also lowers the overall cost of materials, making Option 2 more cost-effective. Additionally, using less timber reduces the environmental impact, enhancing the sustainability of the structure. Therefore, Option 2 is the preferred solution due to its efficiency, cost-effectiveness and sustainability.

## 5.3 Final results

The final results of the structural analysis,

considering the implemented improvements, are summarized in the tables below. The first table presents the unity checks for the outer beams and diagonals, while the second table presents the unity checks for the inner beams.

The unity checks for the outer beams and diagonals, as shown in Table 5, indicate that all stress conditions are within acceptable limits. Specifically, the highest unity check is 0.74 for the Serviceability Limit State (SLS), which is below the critical threshold of 1.0. This confirms that the outer beams and diagonals meet both the safety and serviceability requirements.

*Table 5: Unity check outer members and diagonals*

Due to	Unity Check [-]
<b>Moment</b>	0.25
<b>Compression</b>	0.11
<b>Buckling</b>	0.3
<b>Bending + compression (y dominant)</b>	0.16
<b>Bending + compression (z- dominant)</b>	0.12
<b>Bending + tension (y- dominant)</b>	0.38
<b>Bending + tension (z- dominant)</b>	0.18
<b>SLS</b>	0.84

The unity checks for the inner beams, as shown in Table 6, are also within acceptable limits. The highest unity check for these members is 0.84 for the

Serviceability Limit State (SLS). This further confirms that the improvements made to the structure ensure compliance with all relevant safety and serviceability standards.

*Table 6: Unity check inner members*

Due to	Unity Check [-]
<b>Moment</b>	0.41
<b>Compression</b>	0.27
<b>Buckling</b>	0.32
<b>Bending + compression (y dominant)</b>	0.51
<b>Bending + compression (z- dominant)</b>	0.27
<b>Bending + tension (y- dominant)</b>	0.45
<b>Bending + tension (z- dominant)</b>	0.25
<b>SLS</b>	0.74

Overall, the final results demonstrate that the structure, with the proposed modifications, meets the necessary criteria for both safety and serviceability. The unity checks for all components are well within the acceptable range, indicating a robust and reliable design.

## 7. DISCUSSION

One of the most remarkable aspects of this project was discovering the significant impact that simple diagonal elements can have on the structural performance. I omitted the membrane analysis,

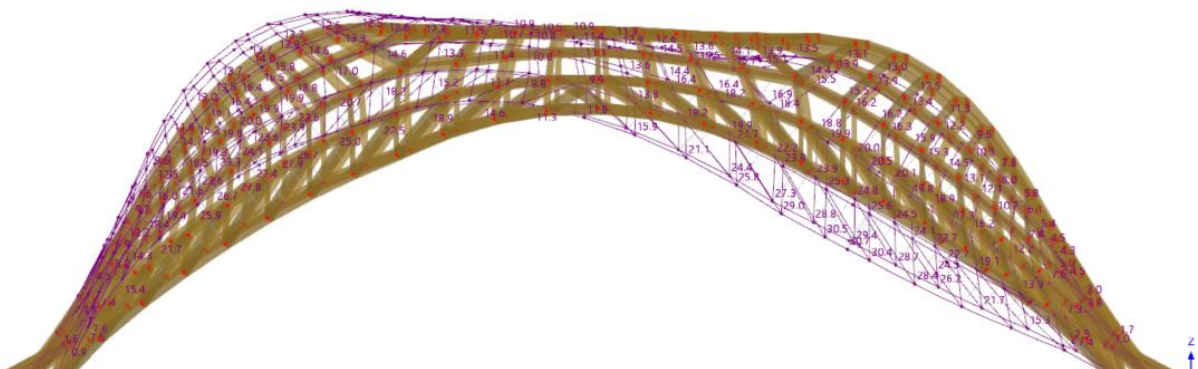


*Figure 19: Deformation final structure [mm]*

which includes basic internal forces, such as  $m_x$ ,  $m_y$ ,  $m_{xy}$ ,  $v_x$ ,  $v_y$ ,  $n_x$ ,  $n_y$  and  $n_{xy}$ , in the RFEM software, due to time constraints. Given more time, I would have incorporated these analyses.

Regarding the applied techniques, the parametric design approach proved to be highly effective. It allowed for easy modifications and adjustments, significantly enhancing the flexibility and efficiency of the design process

## 8. CONCLUSION

The paper gives a full investigation into the design and structural analysis of a timber shell construction using RFEM. The first modelling and analysis revealed several locations where the structure failed to fulfil the necessary safety and serviceability standards, particularly in terms of bending, combined bending and compression, combined bending and tension and maximum deformations.

To address these concerns, two improved solutions were presented. Option 1 increased cross-sectional dimensions to 80 mm by 180 mm, improving structural performance but resulting in a greater timber volume of 5.42 m<sup>3</sup>. Option 2, which required enlarging the borders to 80 mm by 160 mm, adding diagonals of the same size and expanding the interior members to 60 mm by 120 mm, proved more efficient. This solution lowered the timber volume to 3.42 m<sup>3</sup>, assuring material efficiency and cost-effectiveness while preserving structural integrity and sustainability.

The final analysis of the modified structure revealed that all unity checks for both the outer and inner beams were well within acceptable limits, indicating that the design changes adequately addressed the initial shortcomings. Maximum deformations were greatly minimised, ensuring compliance with serviceability standards.

Finally, the study emphasises the necessity of iterative design and analysis in creating a safe, efficient and sustainable timber shell construction. The use of RFEM enabled extensive analysis and optimisation, ensuring that the final design not only met, but exceeded, the needed criteria. Option 2 stands out as the best solution because it strikes the perfect blend of structural performance, material

efficiency, cost-effectiveness and environmental sustainability. This article emphasises timber's versatility and sustainability in current structural engineering.

## ACKNOWLEDGMENTS

I would like to express my sincere gratitude to A. Borgart and P. Eigenraam for their invaluable guidance and knowledge throughout this study. Their expertise and support were instrumental in the successful completion of this paper.

## REFERENCES

- [1] **A. Adelzadeh**, timber shell system fuses polygonal framing & reciprocal bracing for efficient construction, designboom.com, 2023, URL: <https://www.designboom.com/design/timber-shell-system-polygonal-framing-reciprocal-bracing-efficient-construction-reciprocal-shell-10-20-2023/>
- [2] **“Materialdistrict.com”**, a bamboo-timber grid shell, materialdistrict.com, 2023, URL: <https://materialdistrict.com/article/a-bamboo-timber-grid-shell/>

## APPENDIX

### Appendix 1: List of symbols

Symbol	Description	Unit
$\sigma_{m,0,d}$	Design bending stress	N/mm <sup>2</sup>
$M_d$	Design moment	kNm
$b$	Width of the cross section	mm
$h$	Height of the cross section	mm
$\sigma_{c,0,d}$	Design compressive stress	N/mm <sup>2</sup>
$N$	Normal force	kN
$f_{c,0,k}$	Characteristic compressive strength	N/mm <sup>2</sup>

$f_{c,0,d}$	Design compressive strength	N/mm2
$f_{t,0,k}$	Characteristic tensile strength	N/mm2
$f_{t,0,d}$	Design tensile strength	N/mm2
$\gamma_m$	Partial safety factor material	-
$k_{mod}$	Modification factor	-
$r$	Radius of gyration	-
$I$	Moment of inertia	mm4
$E_{0.05}$	5 <sup>th</sup> percentile modulus of elasticity	N/mm4
$\lambda$	Slenderness ratio	-
$\lambda_{rel}$	Relative slenderness ratio	-
$k$	Buckling factor	-
$k_c$	Critical buckling factor	-
$\beta$	Empirical buckling factor	-
$d_{structure}$	Actual displacement	mm
$d_{allowed}$	Allowable displacement	mm
$UC$	Unity Check	-
$\sigma_{t,0,d}$	Design tensile stress	N/mm2
$\sigma_{m,y,d}$	Bending stress in y-direction	N/mm2
$\sigma_{m,z,d}$	Bending stress in z-direction	N/mm2
$k_m$	Interaction factor	-

Option 1

Option 2: Outer

Option 3: Inner

Strength Class	C24		Strength Class	C24	
$f_{cmk}$	24	[N/mm2]	$f_{cmk}$	24	[N/mm2]
$E_{0,mean}$	11000	[N/mm2]	$E_{0,mean}$	11000	[N/mm2]
$E_{0,05}$	7400	[N/mm2]	$E_{0,05}$	7400	[N/mm2]
$f_{ctk}$	21	[N/mm2]	$f_{ctk}$	21	[N/mm2]
Cross section	100x50		Cross section	120x60	
$h$	160	[mm]	$h$	120	[mm]
$b$	80	[mm]	$b$	60	[mm]
$k_h$	0.99	[-]	$k_h$	1.05	[-]
$k_{mod}$	0.80	[-]	$k_{mod}$	0.80	[-]
$\gamma_{m,m}$	1.30	[-]	$\gamma_{m,m}$	1.30	[-]
$f_{mod}$	14.58	[N/mm2]	$f_{mod}$	15.44	[N/mm2]
$f_{cod}$	12.92	[N/mm2]	$f_{cod}$	12.92	[N/mm2]
<b>ULS</b>			<b>ULS</b>		
$M_{max}$	2.03	[kNm]	$M_{max}$	0.54	[kNm]
$\sigma_{max}$	5.35	[N/mm2]	$\sigma_{max}$	5.42	[N/mm2]
$\sigma_{mod}$	0.41	[N/mm2]	$\sigma_{mod}$	0.25	[N/mm2]
<b>Bending compression</b>	<b>Max M</b>		<b>Bending compression</b>	<b>Max M</b>	
$N_{max}$	44.80	[kN]	$N_{max}$	10.57	[kN]
$\sigma_{mod}$	3.50	[N/mm2]	$\sigma_{mod}$	1.47	[N/mm2]
$M_y$	2.03	[kNm]	$M_y$	0.29	[kNm]
$\sigma_{mod,y}$	5.35	[N/mm2]	$\sigma_{mod,y}$	2.01	[N/mm2]
$M_z$	0.09	[kNm]	$M_z$	0.02	[kNm]
$\sigma_{mod,z}$	0.53	[N/mm2]	$\sigma_{mod,z}$	0.28	[N/mm2]
$UC_{bend\_comp\_y\_primary}$	0.51	[-]	$UC_{bend\_comp\_y\_primary}$	0.16	[-]
$UC_{bend\_comp\_z\_primary}$	0.40	[-]	$UC_{bend\_comp\_z\_primary}$	0.12	[-]
$UC_{compression\_only}$	0.27	[-]	$UC_{compression\_only}$	0.11	[-]
<b>Bending tension</b>			<b>Bending tension</b>		
$N_{max}$	54.50	[kN]	$N_{max}$	23.42	[kN]
$\sigma_{mod}$	4.26	[N/mm2]	$\sigma_{mod}$	2.95	[N/mm2]
$M_y$	0.17	[kNm]	$M_y$	0.03	[kNm]
$\sigma_{mod,y}$	0.50	[N/mm2]	$\sigma_{mod,y}$	0.21	[N/mm2]
$M_z$	0.30	[kNm]	$M_z$	0.09	[kNm]
$\sigma_{mod,z}$	1.76	[N/mm2]	$\sigma_{mod,z}$	1.25	[N/mm2]
$UC_{bend\_tens\_y\_primary}$	0.45	[-]	$UC_{bend\_tens\_y\_primary}$	0.33	[-]
$UC_{bend\_tens\_z\_primary}$	0.25	[-]	$UC_{bend\_tens\_z\_primary}$	0.11	[-]
<b>Buckling</b>			<b>Buckling</b>		
$L_z$	27306667	[mm4]	$L_z$	5649000	[mm4]
$A$	12600	[mm2]	$A$	7200	[mm2]
$r$	46.19	[mm]	$r$	34.64	[mm]
$L_{ef}$	517	[mm]	$L_{ef}$	517	[mm]
$l_{bda}$	11.19	[-]	$l_{bda}$	14.92	[-]
$l_{bda\_rel}$	0.19	[-]	$l_{bda\_rel}$	0.25	[-]
$k$	0.51	[-]	$k$	0.53	[-]
$k_c$	1.02	[-]	$k_c$	1.01	[-]
$UC_{buckling}$	0.32	[-]	$UC_{buckling}$	0.36	[-]

b	100	[mm]	b	120	[mm]
h	50	[mm]	h	60	[mm]
k <sub>h</sub>	1.08	[-]	k <sub>h</sub>	0.95	[-]
k <sub>mod</sub>	0.80	[-]	k <sub>mod</sub>	0.80	[-]
gamma <sub>m</sub>	1.30	[-]	gamma <sub>m</sub>	1.30	[-]
f <sub>mod</sub>	16.02	[N/mm <sup>2</sup> ]	f <sub>mod</sub>	14.03	[N/mm <sup>2</sup> ]
f <sub>cod</sub>	12.92	[N/mm <sup>2</sup> ]	f <sub>cod</sub>	12.92	[N/mm <sup>2</sup> ]
<b>ULS</b>			<b>ULS</b>		
M <sub>max</sub>	2.61	[kNm]	M <sub>max</sub>	2.61	[kNm]
M <sub>max</sub>	2610000.00	[N/mm <sup>2</sup> ]	M <sub>max</sub>	2610000.00	[N/mm <sup>2</sup> ]
sigma <sub>mod</sub>	31.32	[N/mm <sup>2</sup> ]	sigma <sub>mod</sub>	5.42	[N/mm <sup>2</sup> ]
UC <sub>moment</sub>	1.96		UC <sub>moment</sub>	0.38	
<b>Bending compression</b>			<b>Bending compression</b>		
Max M	Max N		Max M	Max N	
N <sub>max</sub>	4.61	6335 [kN]	N <sub>max</sub>	4.61	6335 [kN]
sigma <sub>mod</sub>	0.92	13.91 [N/mm <sup>2</sup> ]	sigma <sub>mod</sub>	0.30	4.50 [N/mm <sup>2</sup> ]
M <sub>y</sub>	2.61	2.42 [kNm]	M <sub>y</sub>	2.61	2.42 [kNm]
sigma <sub>mod,y</sub>	31.32	23.04 [N/mm <sup>2</sup> ]	sigma <sub>mod,y</sub>	5.42	5.63 [N/mm <sup>2</sup> ]
M <sub>z</sub>	0.71	1.06 [kNm]	M <sub>z</sub>	0.71	1.06 [kNm]
sigma <sub>mod,z</sub>	17.04	25.44 [N/mm <sup>2</sup> ]	sigma <sub>mod,z</sub>	3.50	5.23 [N/mm <sup>2</sup> ]
UC <sub>bend_comp_y_primary</sub>	2.71	4.08 [-]	UC <sub>bend_comp_y_primary</sub>	0.56	0.74 [-]
UC <sub>bend_comp_z_primary</sub>	2.44	4.02 [-]	UC <sub>bend_comp_z_primary</sub>	0.52	0.75 [-]
UC <sub>compression_only</sub>	0.07	1.08 [-]	UC <sub>compression_only</sub>	0.02	0.35 [-]
<b>Bending tension</b>			<b>Bending tension</b>		
N <sub>max</sub>	55.30	[kN]	N <sub>max</sub>	55.30	[kN]
sigma <sub>mod</sub>	11.06	[N/mm <sup>2</sup> ]	sigma <sub>mod</sub>	3.44	[N/mm <sup>2</sup> ]
M <sub>y</sub>	2.52	[kNm]	M <sub>y</sub>	2.52	[kNm]
sigma <sub>mod,y</sub>	30.24	[N/mm <sup>2</sup> ]	sigma <sub>mod,y</sub>	5.24	[N/mm <sup>2</sup> ]
M <sub>z</sub>	1.30	[kNm]	M <sub>z</sub>	1.30	[kNm]
sigma <sub>mod,z</sub>	31.20	[N/mm <sup>2</sup> ]	sigma <sub>mod,z</sub>	6.41	[N/mm <sup>2</sup> ]
UC <sub>bend_tens_y_primary</sub>	4.11	[-]	UC <sub>bend_tens_y_primary</sub>	0.97	[-]
UC <sub>bend_tens_z_primary</sub>	4.00	[-]	UC <sub>bend_tens_z_primary</sub>	0.79	[-]
UC <sub>compression_only</sub>	0.65	[-]			
<b>Buckling</b>			<b>Buckling</b>		
L <sub>z</sub>	4166666.7	[mm <sup>4</sup> ]	L <sub>z</sub>	45126667	[mm <sup>4</sup> ]
A	5000	[mm <sup>2</sup> ]	A	15200	[mm <sup>2</sup> ]
r	28.87	[mm]	r	54.95	[mm]
L <sub>ef</sub>	517	[mm]	L <sub>ef</sub>	517	[mm]
l <sub>bda</sub>	17.31	[-]	l <sub>bda</sub>	9.45	[-]
l <sub>bda,rel</sub>	0.30	[-]	l <sub>bda,rel</sub>	0.16	[-]
k	0.55	[-]	k	0.50	[-]
k <sub>c</sub>	1.00	[-]	k <sub>c</sub>	1.03	[-]
UC <sub>buckling</sub>	1.08	[-]	UC <sub>buckling</sub>	0.34	[-]
<b>Deformation</b>			<b>Deformation</b>		
max_def	86.5	[mm]	max_def	15.42	[mm]
d <sub>allowed</sub>	16.67	[mm]	d <sub>allowed</sub>	31.62	[mm]
UC <sub>SLS</sub>	5.19		UC <sub>SLS</sub>	0.423783474	

## Appendix 2: Calculation sheets

From top left to bottom right:

Initial structure



